

## SUPPORTING INFORMATION

### **Janus $\beta$ -PdXY (X/Y = S, Se, Te) Materials with high Anisotropic Thermoelectric Performance**

Mukesh Jakhar<sup>1</sup>, Raman Sharma<sup>2</sup> and Ashok Kumar<sup>1\*</sup>

*<sup>1</sup>Department of Physics, School of Basic Sciences, Central University of Punjab, Bathinda,  
151401, India*

*<sup>2</sup>Department of Physics, Himachal Pradesh University, Shimla, 171005, India*

(January 28, 2023)

\*Corresponding Author:

[ashokphy@cup.edu.in](mailto:ashokphy@cup.edu.in) (Ashok Kumar)

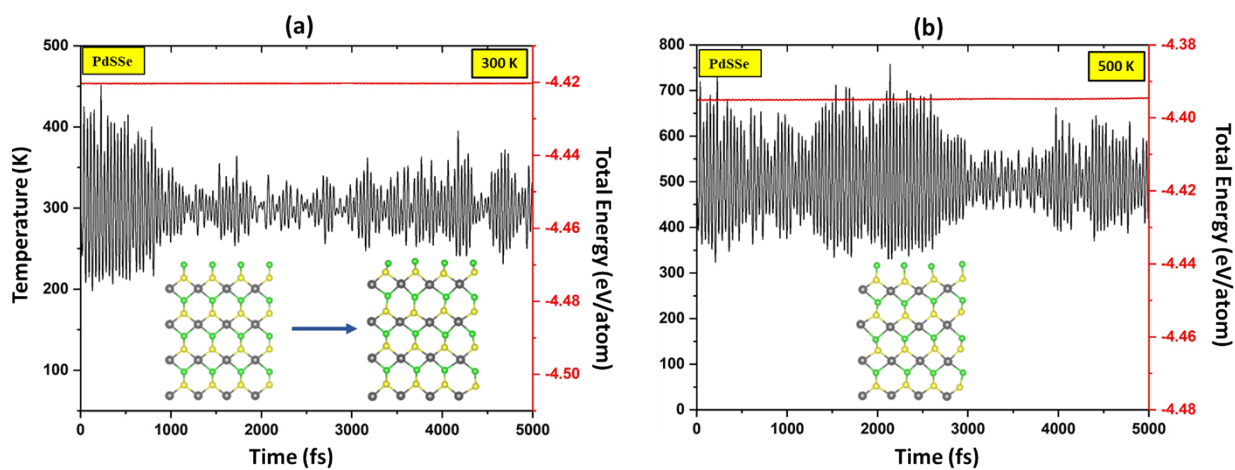


**Fig. S1.** The AIMD total energy (eV/atom) and temperature fluctuations at (a) 300 K, (b) 500 K, with the snapshot of Janus PdSSe monolayer before and after a 5000 fs AIMD simulations.

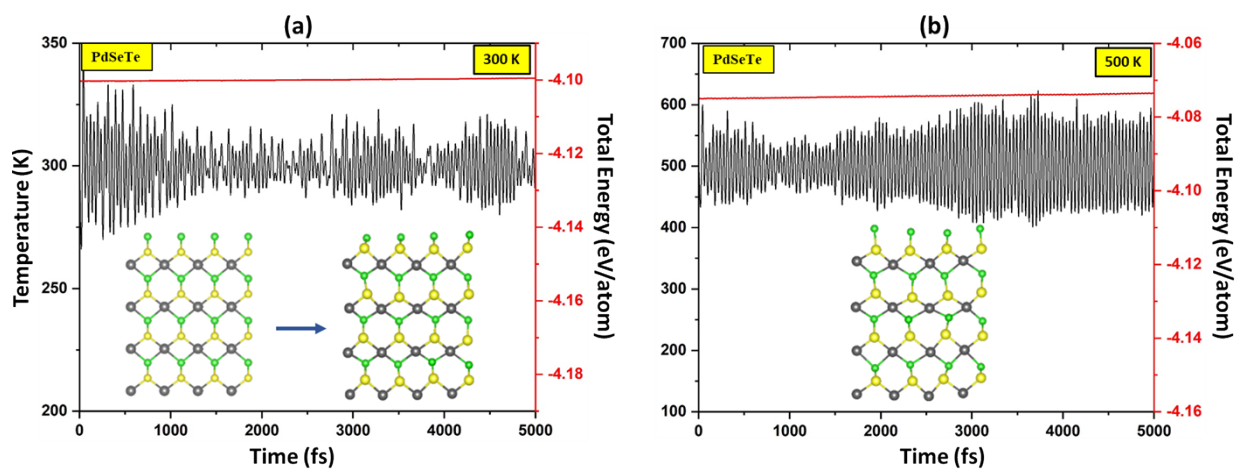


**Fig. S2.** The AIMD total energy (eV/atom) and temperature fluctuations at (a) 300 K, (b) 500 K, with the snapshot of Janus PdSeTe monolayer before and after a 5000 fs AIMD simulations.

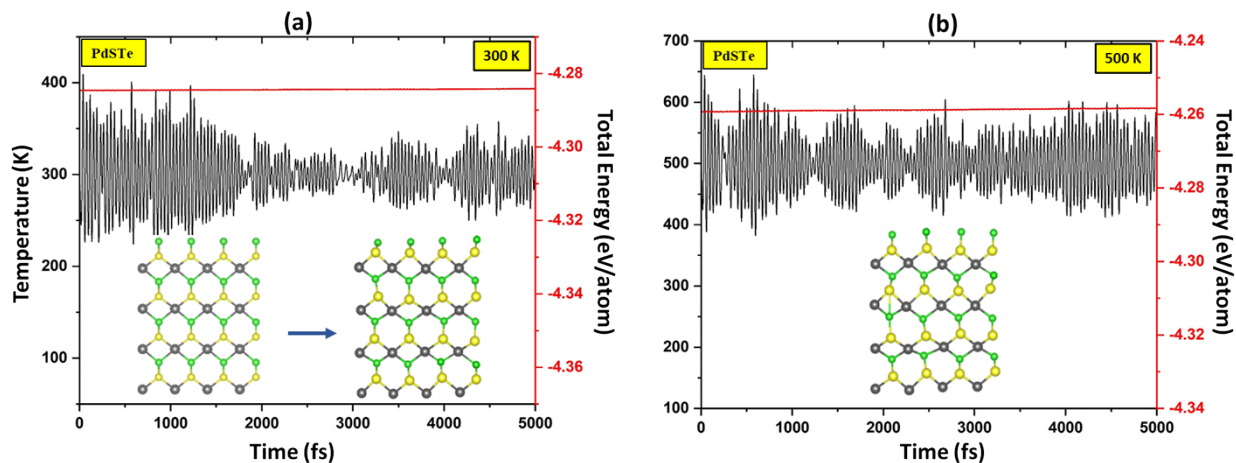


**Fig. S3.** The AIMD total energy (eV/atom) and temperature fluctuations at (a) 300 K, (b) 500 K, with the snapshot of Janus PdSTe monolayer before and after a 5000 fs AIMD simulations.

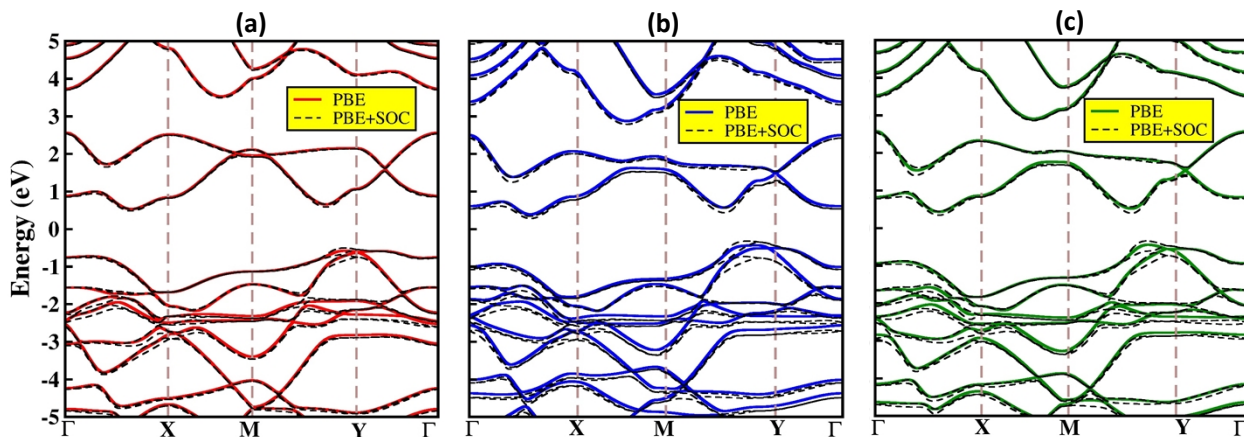


**Fig. S4:** The calculated electronic structures using PBE and PBE+SOC level of theory for Janus (a) PdSSe (b) PdSeTe and (c) PdSTe monolayers.

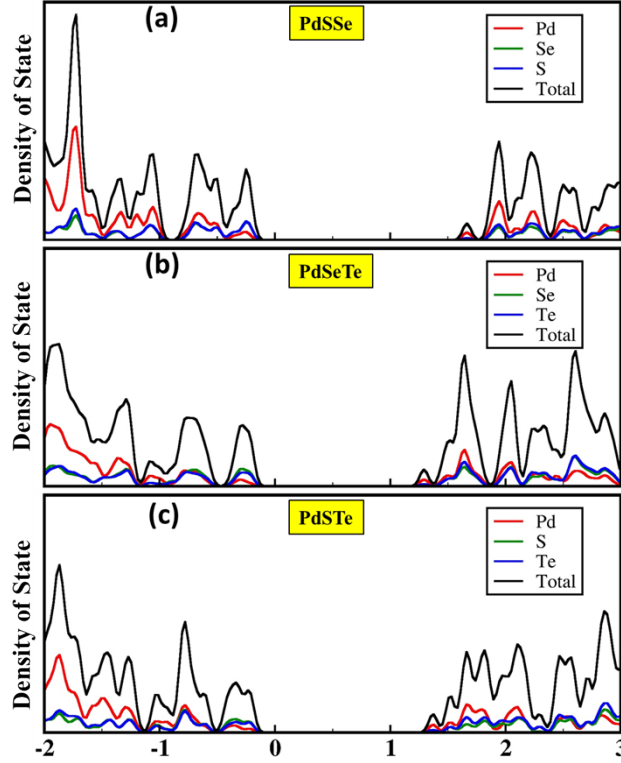


**Fig. S5:** The calculated PDOS using HSE06 level for Janus (a) PdSSe (b) PdSeTe and (c) PdSTe monolayers.

**Table S1:** Janus  $\beta$ -PdXY (X, Y =S, Se, Te) monolayers: The effective mass ( $m^*$ ), average effective mass ( $m_a^*$ ), elastic modulus of the material ( $C_{2D}$ ), the deformation potential ( $E_i$ ), charge carrier mobilities ( $\mu_{2D}$ ), dominated LO-phonon frequency ( $\hbar\omega_{LO}$ ), high-frequency ( $\epsilon_\infty$ ) and lattice ( $\epsilon_L$ ) dielectric constants and the electronic relaxation times ( $\tau_e$ ) at 300 K along x and y direction.

Material	Carriers	$m^*$	$m_a^*$	$C_{2D}$ (J/m <sup>2</sup> )	$E_i$ (eV)	$\mu_{2D}$ (cm <sup>2</sup> V <sup>-1</sup> S <sup>-1</sup> )	$\tau_e$ (ps)	$\epsilon_\infty$	$\epsilon_L$	$\hbar\omega_{LO}$ (meV)
$\beta$ -PdSSe	$p(x)$	1.76	1.83	37.42	1.25	106.02	0.106	4.3	4.6	40.6
	$n(x)$	0.38	0.84	37.42	4.62	78.39	0.016	4.3	4.6	40.6
	$p(y)$	1.91	1.83	22.71	0.76	160.12	0.170	4.0	4.1	40.6
	$n(y)$	1.86	0.84	22.71	3.53	16.37	0.017	4.0	4.1	40.6
$\beta$ -PdSeTe	$p(x)$	0.97	0.55	35.84	4.16	54.46	0.030	6.0	6.3	25.9
	$n(x)$	0.28	1.0	35.84	2.85	225.13	0.035	6.0	6.3	25.9
	$p(y)$	0.32	0.55	11.52	1.02	863.86	0.157	4.9	5.1	25.9
	$n(y)$	3.60	1.0	11.52	3.35	4.03	0.008	4.9	5.1	25.9
$\beta$ -PdSTe	$p(x)$	1.29	0.64	39.2	1.33	1424.79	0.270	6.6	7.1	38.9
	$n(x)$	0.29	1.72	39.2	2.59	167.57	0.027	6.6	7.1	38.9
	$p(y)$	0.32	0.64	13.2	0.5	3618.76	0.658	5.36	5.7	38.9
	$n(y)$	10.23	1.72	13.2	2.5	1.70	0.009	5.36	5.7	38.9

**Table S2:** The electron and hole carrier concentration corresponding to highest ZT value with different temperature along x and y directions for all three Janus PdSeS, PdSeTe and PdSTe monolayer.

Janus System	Temperature	Direction	Carrier Concentration (N)	
			$N_h \times (10^{13})$	$N_e \times (10^{13})$
PdSSe	300	x	4.32	0.78
		y	2.90	0.54
	500	x	6.82	1.42
		y	3.00	0.42
	800	x	0.83	2.30
		y	3.57	0.40
PdSeTe	300	x	2.76	0.42
		y	2.76	0.42
	500	x	2.65	0.71
		y	1.73	0.47
	800	x	2.65	1.03
		y	1.06	4.19
PdSTe	300	x	1.47	0.65
		y	2.88	0.45
	500	x	2.12	0.90
		y	2.12	0.90
	800	x	1.83	0.89
		y	1.83	0.56

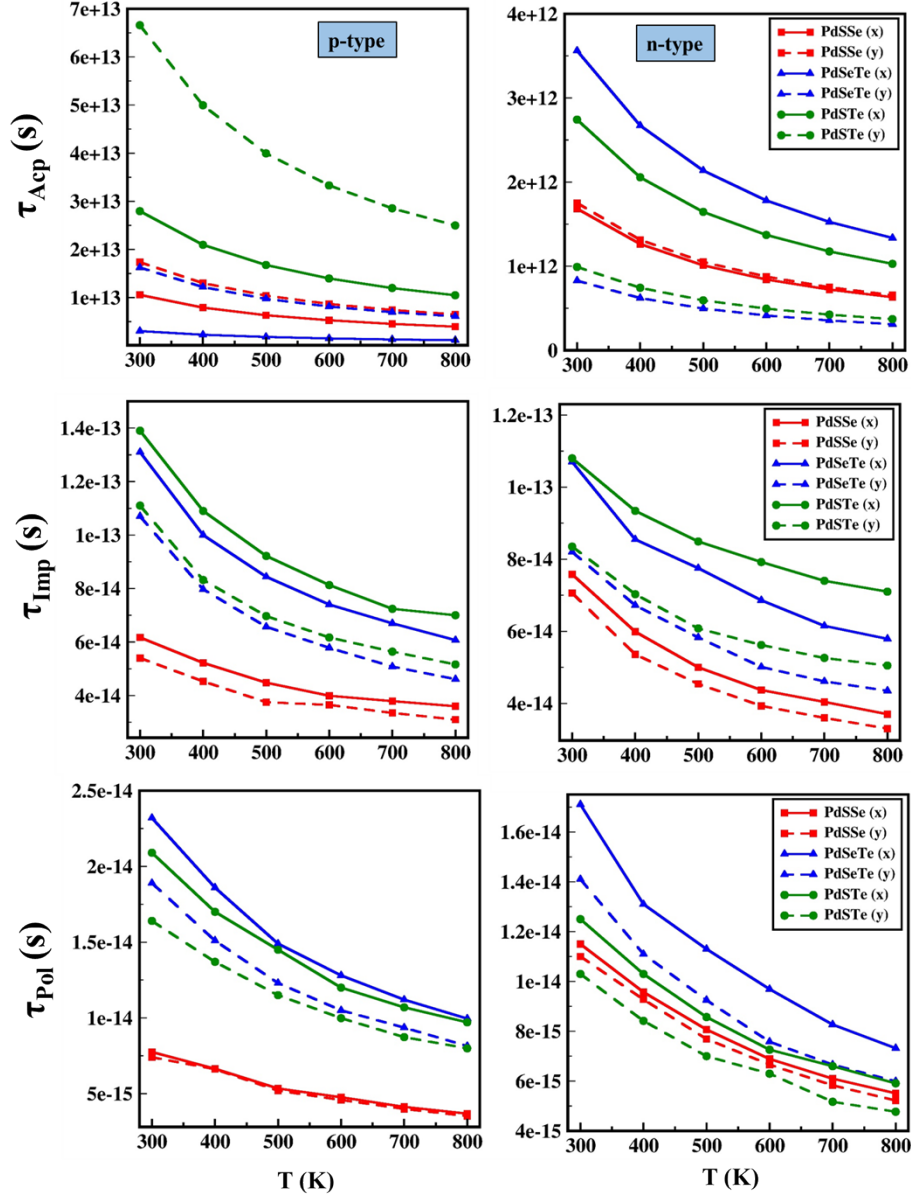


**Fig. S6.** The calculated electronic relaxation time with acoustic phonon scattering ( $\tau_{Acp}$ ), impurity scattering ( $\tau_{Imp}$ ), and polarized phonon scattering ( $\tau_{Pol}$ ) p-type and n-type Janus  $\beta$ -PdXY (X/Y = S, Se, Te) monolayers along the x and y-direction

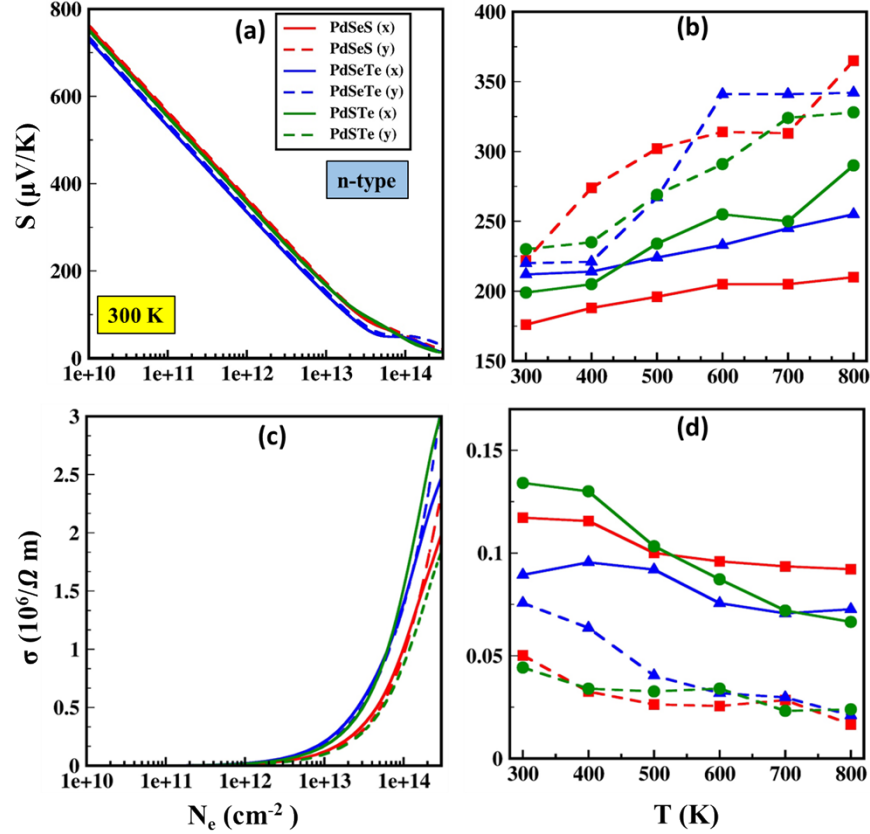


**Fig. S7.** The calculated Seebeck coefficient ( $S$ ) and electrical conductivity ( $\sigma$ ) as a function of (a, c) carrier concentration ( $N_e$ ) at 300 K and (b, d) temperature ( $T$ ) for n-type Janus  $\beta$ -PdXY ( $X/Y = S, Se, Te$ ) monolayers along x and y direction.

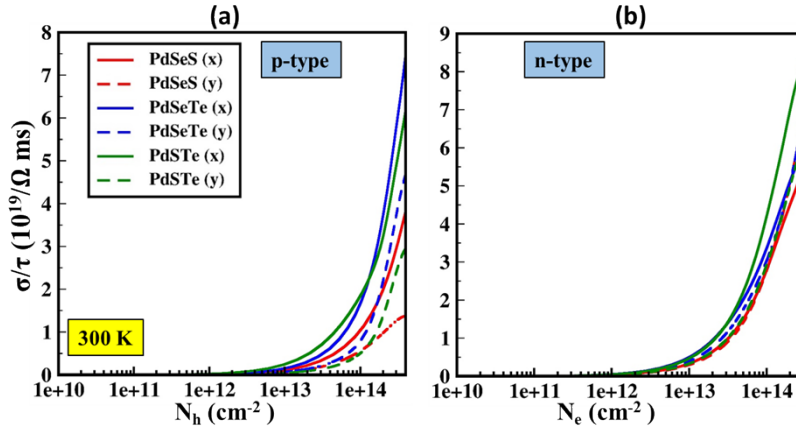


**Fig. S8.** The calculated electrical conductivity ( $\sigma/\tau$ ) as a function of carrier concentration ( $N_h$ ) at 300 K for p-type Janus  $\beta$ -PdXY ( $X/Y = S, Se, Te$ ) monolayers along x and y direction.

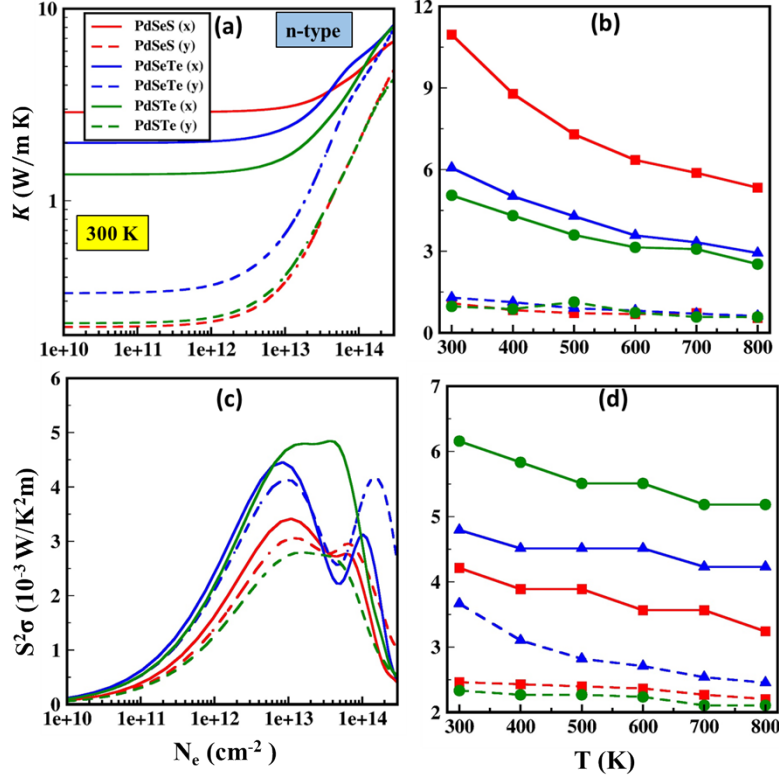


**Fig. S9.** The calculated total conductivity (K) and power factor ( $S^2\sigma$ ) as a function of (a, c) carrier concentration ( $N_e$ ) at 300 K and (b, d) temperature (T) for n-type Janus  $\beta$ -PdXY (X/Y =S, Se, Te) monolayers along x and y direction.

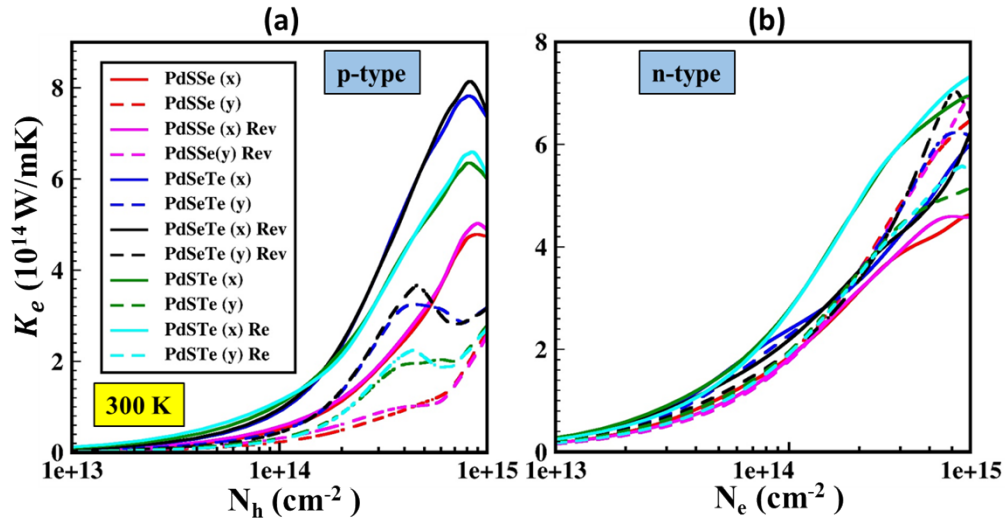


**Fig. S10.** The calculated electronic thermal conductivity and revised electronic thermal conductivity (Rev) at 300 K for (a) p and (b) n-type doped Janus  $\beta$ -PdXY (X/Y =S, Se, Te) monolayers along x and y-direction.

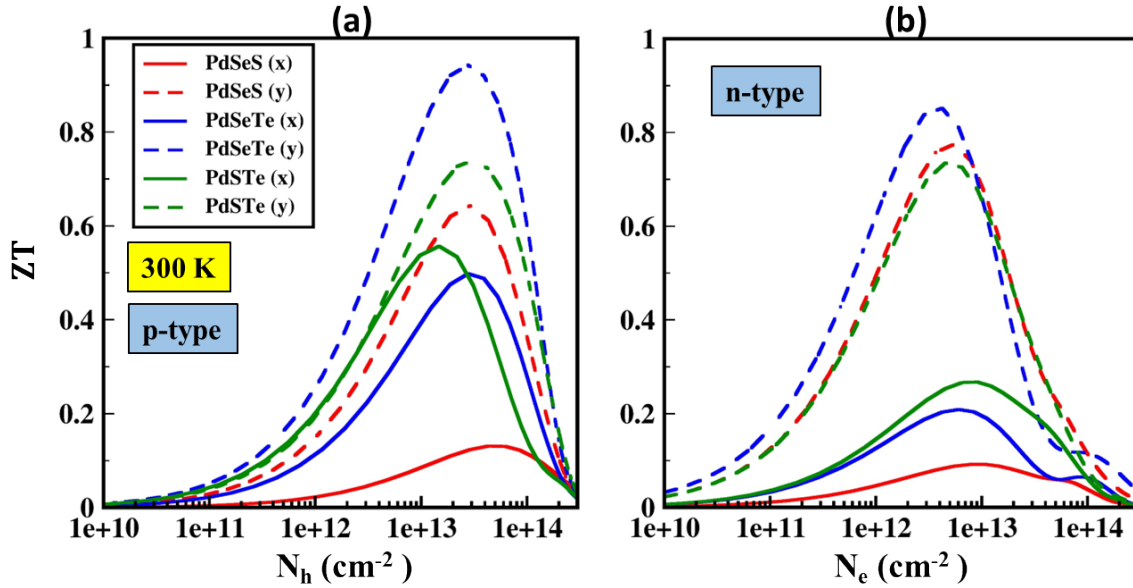


**Fig. S11.** The calculated figure of merit ( $ZT$ ) as a function of carrier concentration ( $N_e$ ) at 300 K for (a) p and (b) n-type doped Janus  $\beta$ -PdXY ( $X/Y = S, Se, Te$ ) monolayers along x and y-direction.

**Table S3:**  $ZT$  and thermal conductivity values of TMDs Janus monolayer at 300 K.

Systems	Lattice Thermal Conductivity X(Y)	Figure of Merit (ZT) at 300 K	Reference
Janus $\beta$ -PdSeS	10.47 (1.60)	0.77	This Work
Janus $\beta$ -PdSeTe	5.86 (0.94)	0.86	This Work
Janus $\beta$ -PdSTe	4.43 (0.77)	0.71	This Work
$\beta$ -PdS <sub>2</sub>	40.58 (7.13)	-	This Work
$\beta$ -PdSe <sub>2</sub>	4.42 (1.47)	-	This Work
$\beta$ -PdTe <sub>2</sub>	6.80 (3.11)	-	This Work
Janus H-PdSSe	10.65	0.09	1
Janus H-PdSTe	5.45	0.26	1
Janus H-PdSeTe	4.02	0.98	1
Janus H-PtSSe	36.19	0.37	1
Janus H-PtSTe	20.56	0.26	1
Janus H-PtSeTe	14.47	0.91	1
Penta-PdS <sub>2</sub>	4.34 (12.48)	0.85	2
Penta-PdSe <sub>2</sub>	2.91 (6.62)	1.18	2
Penta-PdTe <sub>2</sub>	1.42 (5.90)	2.42	2
WS <sub>2</sub>	-	0.006	3
WSe <sub>2</sub>	-	0.138	4
Janus WSSe	-	0.013	3
Janus WSTe	-	0.742	3

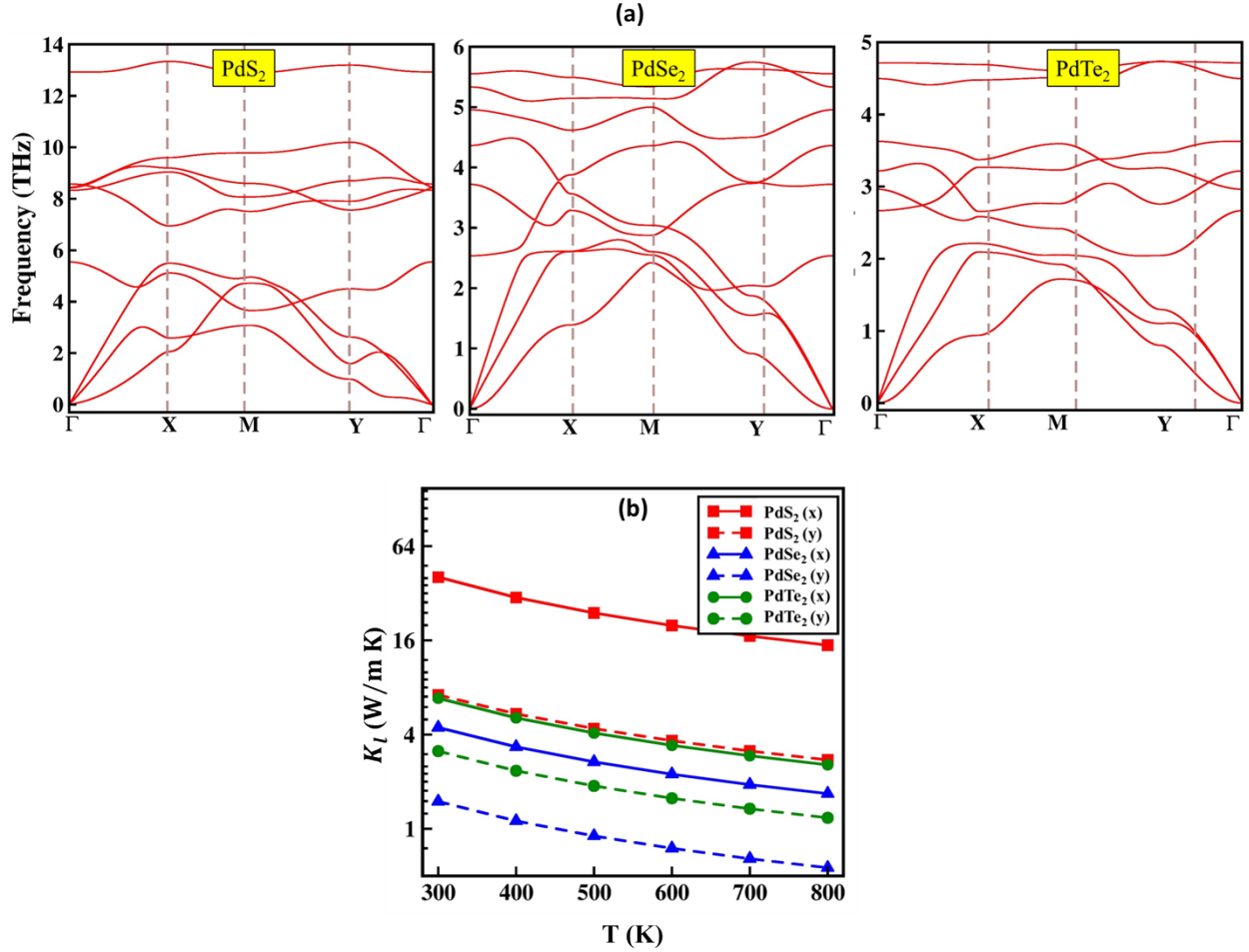


**Fig. S12** The calculated (a) phonon dispersion curves and (b) lattice thermal conductivity for  $\beta$ -PdX<sub>2</sub> (X=S, Se, Te) monolayer.

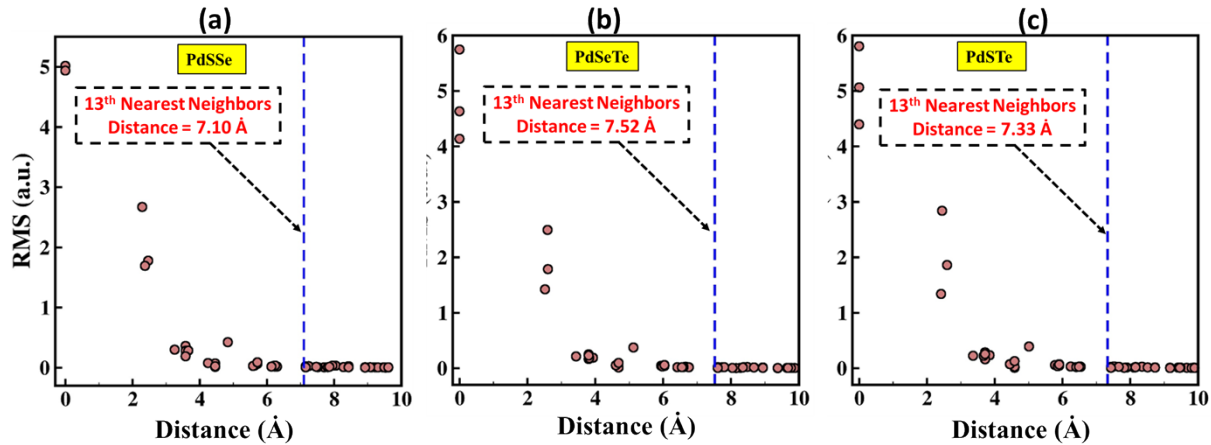
### Convergence Details for Lattice thermal conductivity

In this work, the convergence of thermal conductivity is verified based on the analysis of interatomic interactions. Therefore, the  $r_{\text{cut}}$  off is determined by analyzing the root mean square (RMS) of the elements of the second-order IFCs according to the work of Qin and Hu<sup>5</sup>, as follows:

$$RMS(\phi_{ij}) = \left[ \frac{1}{9} \sum_{\alpha, \beta} (\phi_{ij}^{\alpha\beta})^2 \right]^{1/2}$$

Where  $\phi_{ij}$  is the second-order IFCs between atom  $i$  and  $j$ , and  $ij$  is the harmonic response of the force acting on atom  $i$  ( $\alpha$ -direction) resulting from the displacement of atom  $j$  ( $\beta$ -direction).

As shown in Fig. S13, as the distance increases, the interactions in the plane decrease monotonically. We chose the  $r_{\text{cut}}$  off of 7.10 Å, 7.52 Å and 7.33 Å with 13<sup>th</sup> nearest neighbor atoms for all the Janus PdSeS, PdSeTe and PdSTe monolayers, respectively, combined with different q-grid sizes to make the convergence tests of  $K_l$ . Hence, Considering the results of RMS ( $\Phi_{ij}$ ) and convergence tests and the computational cost, at least a  $r_{\text{cut}}$  off (distance) of 7.10 Å, 7.52 Å and 7.33 Å is required for obtaining converge Janus PdSeS, PdSeTe and PdSTe monolayers respectively (Fig. S13 (a-c)).



Fi

**g. S13.** The relationship between the RMS and cutoff distance reveals the long-distance interatomic interactions for Janus (a) PdSSe (b) PdSeTe (c) PdSTe monolayers.

Next, by considering the lattice thermal conductivity ( $K_l$ ) at 300 K as an example, as shown in Fig. S14 (a-f), we also tested the convergence of  $K_l$  with the Q-grid and gaussian smearing. The Q-grid convergence results show that after the high Q-grid of  $30 \times 30 \times 1$ , there is negligible fluctuation in  $K_l$  the value proves the rationality of selecting the Q-grid for all three Janus PdSeS, PdSeTe and PdSTe monolayers. However, the gaussian smearing is considered by the parameter scaleboard in ShengBTE code<sup>6</sup>. We choose the scaleboard equal to 1.0 in this study (Fig. S14 (d-f)) for all Janus monolayers, which is also recommended in many studies for getting accurate scattering rates<sup>6</sup>.

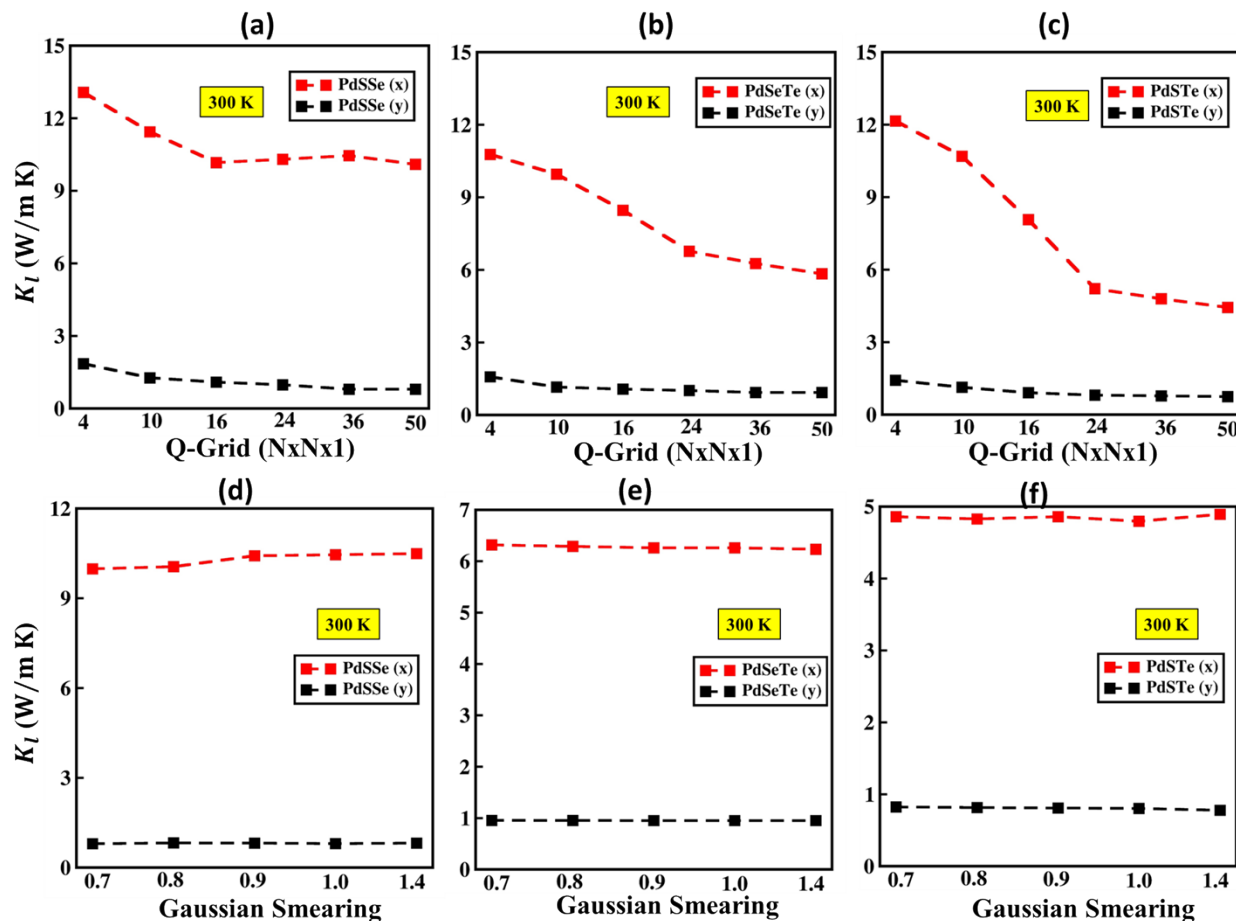


**Fig. S14** The convergence test of the thermal conductivity with the variation in the Q-grid and Gaussian Smearing for Janus (a, d) PdSSe (b, c) PdSeTe (c, f) PdSTe monolayers.

## References

1. W.-L. Tao, J.-Q. Lan, C.-E. Hu, Y. Cheng, J. Zhu and H.-Y. Geng, *Journal of Applied Physics*, 2020, **127**, 035101.
2. D. Qin, P. Yan, G. Ding, X. Ge, H. Song and G. Gao, *Scientific reports*, 2018, **8**, 1-8.
3. A. Patel, D. Singh, Y. Sonvane, P. Thakor and R. Ahuja, *ACS applied materials & interfaces*, 2020, **12**, 46212-46219.
4. S. Kumar and U. Schwingenschlogl, *Chemistry of Materials*, 2015, **27**, 1278-1284.
5. G. Qin and M. Hu, *npj Computational Materials*, 2018, **4**, 1-6.
6. W. Li, J. Carrete, N. A. Katcho and N. Mingo, *Computer Physics Communications*, 2014, **185**, 1747-1758.